13

Nonlinear $\mathcal{H}_\infty$ Control Applied to Biped Robots

Adriano A. G. Siqueira, Marco H. Terra and Leonardo Tubota
University of São Paulo, São Carlos, São Paulo
Brazil

1. Introduction

Researches on biped robots have been the focus of many universities and industries around the world Hirukawa et al. (2004). The challenges in the study of this kind of system, beyond, of course, the stability of the walking, are strongly coupled with nonlinearities and with the occurrence of discontinuities in the joint variables when the swing foot touches the ground.
Control strategies for biped robots can be classified in two categories according to the degree of actuation of the joints: control strategies based on the Zero Moment Point (ZMP), which is considered a fully actuated system, and control strategies based on the dynamic passive walking, which the few (or even none) degrees of actuation are used.
The ZMP criterion to evaluate biped robot stability was initially proposed by Vukobratovic & Juricic (1969). Shortly, the ZMP is the point in the ground where the resultant of reaction moments are null. If the ZMP is inside the support polygon, defined by the contact points of the robot with the ground, the walking is stable. In Huang et al. (2001), it is presented one of many trajectory generators for biped robots taking into account the ZMP criterion. Specific points of the ankle and hip trajectories are defined according to the desired step length and duration. The minimization of a functional related to the ZMP gives the desired trajectories, which, tracked trough the actuation of all joints, generate a stable movement of the biped robot.
On the other hand, the movement of passive walking robots is created by the action of the gravity in an inclined surface, without any joint actuation. In this case, when the foot of the swing leg touches the ground there is energy spending which is compensated by the ground slope. A passive walking occurs when the joint positions and velocities at the final of the step are identical to the initial conditions. The movement generated can be characterized as periodic movement or, in terms of nonlinear systems analysis, a limit cycle.
The problems related to passive dynamic walking are more complex than to the static case, however, the dynamic walking gives higher velocities, bigger energy efficiency, and a smooth and anthropomorphic movement. A scientific research on these mechanisms starts with McGeer (1990). McGeer shows that a fully no actuated biped robot, and hence no controllable, can present a stable walking on an inclined surface for some dynamic parameter selections. In Asano et al. (2005) the passive walk is used in order to define a control law that uses the energy trajectory as trajectory reference, which is time independent (standard trajectories which depend on state variables are time dependent) and it assures the robustness of the system. This is the motivation to consider the passive walk as the best model in terms of energy consumption.

However, the basin of attraction of the limit cycle for passive walking is generally small and sensitive to disturbances and ground slope variations. For example, in Goswani et al. (1998), bifurcations with period duplication occur when the ground slope varies from 3° to 5°. In Spong & Bhatia (2003), it is shown that the walking can be made slope invariant for a bidimensional biped robot without knees and torso, and with actuators on the hip and ankles, considering a controller based on gravity compensation. It is also shown that the basin of attraction and the robustness can be increased using an energy-based controller. In Bhatia & Spong (2004), this procedure is extended to a bidimensional biped robot with knees and torso. Gravity compensation and energy-based controllers are also presented in Asano & Yamakita (2001) for passive walking robots.

In this chapter, it is used a control strategy for passive walking robots to increase the robustness against external disturbances based on nonlinear $\mathcal{H}_\infty$ controllers. They are based on linear parameter varying (LPV) representation of the biped robot. This kind of approach has been applied to fully actuated and underactuated robot manipulators Siqueira & Terra (2002; 2004). The objective, as in Bhatia & Spong (2004), is to apply the robust controller to leads back the robot to the basin of attraction of the limit cycle. We consider that the robot leaves it due to the disturbances. In this way, the period of application of the controller is minimal and the main characteristic of passive walking (energy save) is preserved.

The biped robot considered here, in addition to knees and torso of the robot presented in Bhatia & Spong (2004), has feet. For biped robots with feet, the time instant when the foot rotates around the toes can be determined by the Foot Rotation Indicator (FRI), described in Goswani (1999). The FRI is a point in the ground surface where the resultant ground reaction force would have to act to keep the foot stationary. In Choi & Grizzle (2005), the authors consider a biped robot with feet and use the FRI as control variable in the procedure to find the zero dynamics of the system proposed in Westervelt et al. (2003). Here, the FRI is also used as control variable to provide to the biped robot an anthropomorphic walking.

This chapter is organized as follows: in Section 2, the dynamic model of the biped robot, considering the foot rotation, the knee strike, and the ground collision, is presented; in Section 3.2, the robust dynamic walking control strategy using the nonlinear $\mathcal{H}_\infty$ control is proposed; and in Section 4, the results obtained from simulation are shown.

2. Dynamic Model of 2D Biped Robots

In this section we present the dynamic model of a planar walking robot, including the swing and ground collision phases. These phases are characterized, respectively, by having the robot only one foot or both feet in contact with the ground. Consider a biped robot with a torso, knees and feet, Figure 1. The overall system has nine degrees of freedom (DOF), corresponding to two DOF of the Y-Z plane, three DOF of each leg, and one DOF of the torso. The biped robot moves over a planar surface with inclination ϕ with relation to the inertial coordinate system.

The robot configuration is described by the angles: q_1 (foot of the stance leg), q_2 (stance leg), q_3 (torso), q_4 (thigh of the swing leg), q_5 (shank of the swing leg), and q_6 (foot of the swing leg). The generalized coordinate q_1 is defined as absolute value with relation to the horizontal axis Y and the remaining angles are defined as relative value to the previous link. The parameters mass (m), length (l), center of mass (c), and inertia momentum with relation to the center of mass (I) of each link are shown in Table 1, where the indexes $i = (1, \cdots, 6)$ are related to the foot of the stance leg, stance leg, torso, thigh of the swing leg, shank of the swing leg, and foot of the swing leg, respectively. The parameters in Table 1 correspond to the values of the

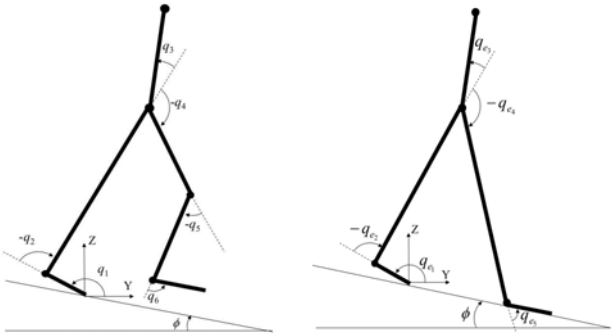

(a) (b)

Fig. 1. a) Bidimensional biped robot with feet. b) Ground collision model.

bidimensional experimental robot RABBIT described in Chevallereau et al. (2003), except the values related to the feet, since RABBIT has no feet. The robot motion in the sagittal plane is divided in two phases: the swing phase and the ground collision phase.

2.1 Swing phase

The swing phase is considered in this chapter as consisting of three sub-phases: before the foot rotation, after the foot rotation and before the knee strike, and after the knee strike. During the first sub-phase, before the foot rotation, the foot link is parallel to the ground and its angular velocity is zero. The change from this phase to the phase of foot rotation around the toe occurs when the Foot Rotation Indicator (FRI) point is outside the foot support area.

The FRI definition was first described in Goswani (1999), as the point in the ground surface where the resultant ground reaction force would have to act to keep the foot stationary. The FRI has some important properties for the control of a biped robot:

- The FRI indicates the occurrence of foot rotation and its direction;
- The location of the FRI indicates the amount of unbalanced moment on the foot;
- The minimum distance between the support polygon and the FRI is a measurement of the stability margin, since that the FRI is inside of the support polygon.

In other words to keep the foot stationary, the FRI must remain inside the foot support area. The FRI incorporates the biped robot dynamics, differently from the ground projection of the center of mass, that represents a static characteristic. The FRI is also different from the center of pressure, known as the zero moment point (ZMP). The ZMP is a point in the ground surface where the resultant ground reaction force is actually applied. Hence, the ZMP never leaves the foot support area, whereas the FRI does so. When the point of application of the resultant ground reaction force is inside the foot support area, the FRI and ZMP are coincident. In a

Parameter	Value	Unit	Parameter	Value	Unit
m_1	$0,5$	kg	c_1	$0,05$	m
m_2	10	kg	c_2	$0,28$	m
m_3	20	kg	c_3	$0,2$	m
m_4	$6,8$	kg	c_4	$0,163$	m
m_5	$3,2$	kg	c_5	$0,128$	m
m_6	$0,5$	kg	c_6	$0,05$	m
l_1	$0,1$	m	I_1	$0,329$	kg.m^2
l_2	$0,8$	m	I_2	$2,06$	kg.m^2
l_3	$0,625$	m	I_3	$1,42$	kg.m^2
l_4	$0,4$	m	I_4	$0,899$	kg.m^2
l_5	$0,4$	m	I_5	$0,878$	kg.m^2
l_6	$0,1$	m	I_6	$0,329$	kg.m^2

Table 1. Biped Robot Parameters.

three-dimensional biped robot, the coordinates of the FRI in the X-Y plane can be obtained as:

$$x_{FRI} = \frac{m_1 x_{c_1} g + \sum_{i=2}^{n} m_i x_{c_i}(\ddot{z}_{c_i} + g) - \sum_{i=2}^{n} m_i z_{c_i} \ddot{x}_{c_i} - \sum_{i=2}^{n} (\dot{H}_{c_y})_i}{m_1 g + \sum_{i=2}^{n} m_i (\ddot{z}_{c_i} + g)},$$
$$y_{FRI} = \frac{m_1 y_{c_1} g + \sum_{i=2}^{n} m_i y_{c_i}(\ddot{z}_{c_i} + g) - \sum_{i=2}^{n} m_i z_{c_i} \ddot{y}_{c_i} - \sum_{i=2}^{n} (\dot{H}_{c_x})_i}{m_1 g + \sum_{i=2}^{n} m_i (\ddot{z}_{c_i} + g)}, \quad (1)$$

where g is the gravity acceleration, x_{c_i} and y_{c_i} are the position coordinates of the center of mass of the link i, $\ddot{x}_{c_i}$, $\ddot{y}_{c_i}$ and $\ddot{z}_{c_i}$ are the acceleration coordinates of the center of mass of the link i and $(\dot{H}_{c_x})_i$ and $(\dot{H}_{c_y})_i$ are the derivative of the angular momentum around the center of mass of the link i. As we are working with a planar biped robot in this chapter, if y_{IRP} in Eq. 1 is above 0, the foot rotation occurs.

The foot rotation occurs in the human being due to the application of a torque around the ankle joint at the end of the foot stance phase. Trying to reproduce this natural behavior on the biped robot considered in this chapter, a torsional spring is introduced on the ankle joint of the stance leg (joint 2), as shown in the Figure 2.

The function describing the torque applied by the spring, τ_M, with relation to the ankle joint displacement, q_2, is given by

$$\tau_M = K_0 - K_M q_2, \quad (2)$$

where $K_0 > K_M > 0$ are control design parameters. They are adjusted to set the foot rotation instant during the step, Palmer (2002). Before the foot rotation, the spring is compressed and

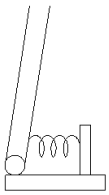

Fig. 2. Representation of a torsional spring in the ankle joint.

stores some part of the dynamic walking energy. During the foot rotation, the stored potential energy is transformed into kinematic one, keeping the dynamic walking.
During the two sub-phases before the knee strike, the dynamic equations of the system are given by:

$$M(q)\ddot{q} + C(q,\dot{q})\dot{q} + g(q) = \tau, \tag{3}$$

where $q = [q_1 \;\; q_2 \;\; q_3 \;\; q_4 \;\; q_5 \;\; q_6]^T$, $M(q) \in \Re^{6\times 6}$ is the inertia matrix, $C(q,\dot{q}) \in \Re^{6\times 6}$ is the Coriolis/centripetal matrix, $g(q) \in \Re^6$ is the gravitational vector, and $\tau = [\tau_1 \;\; \tau_2 \;\; \tau_3 \;\; \tau_4 \;\; \tau_5 \;\; \tau_6]^T$ is the applied torque vector, τ_i $(i = 1, \cdots, 6)$ are the torques in the toe of the stance leg, in the ankle of the stance leg, between the stance leg and the torso, between the stance leg and the thigh of the swing leg, in the knee of the swing leg, and in the ankle of the swing leg, respectively. The shank of the swing leg can move around the knee only to the posterior part of the leg, that is, $q_5 < 0$.
At the instant of the impact, the knee displacement vanishes, $q_5 = 0$. The joint positions do not change during the impact, but the velocities suffer an abrupt change. This event can be modeled by conservation of the angular momentum with relation to the stance leg:

$$M(q^+)\dot{q}^+ = M(q^-)\dot{q}^- - J_i^T\lambda_i, \tag{4}$$

where λ_i are the impulsive forces generated by the impact, q^+ and q^- are the values of q just before and after the knee strike, and $J_i = [0 \;\; 0 \;\; 0 \;\; 0 \;\; 1 \;\; 0]$ is the Jacobian matrix generated by the constraint $J_i\dot{q}^+ = 0$. Since $M(q^+) = M(q^-)$, because $q^+ = q^-$.
From (4), the joint velocities after the impact are computed as function of the velocities just before the impact and of the constraint forces as $\dot{q}^+ = \dot{q}^- - M(q)^{-1}J_i^T\lambda_i$. From the above considerations, the following relation is obtained:

$$J_i\dot{q}^+ = 0 = J_i\dot{q}^- - J_iM(q)^{-1}J_i^T\lambda_i,$$

which results in $\lambda_i = X_i^{-1}J_i\dot{q}^-$ where $X_i = J_iM(q)^{-1}J_i^T$.
After the knee strike, the swing leg remains straight due the constraint forces on the knee generated by a mechanism that locks the joint ($q_5 = 0$). The dynamic equations of the system, considering the constraint forces, are given by:

$$M(q)\ddot{q} + C(q,\dot{q})\dot{q} + g(q) = \tau - J_r^T\lambda_r, \tag{5}$$

where $J_r = [0 \;\; 0 \;\; 0 \;\; 0 \;\; 1 \;\; 0]$. The constraint forces are given by $\lambda_r = -X_r^{-1}J_rM(q)^{-1}(C(q,\dot{q})\dot{q} + g(q))$ where $X_r = J_rM(q)^{-1}J_r^T$.

2.2 Ground Collision Phase

The collision of the foot of the swing leg with the ground can be modeled as a contact between two rigid bodies. It is considered that the heel and the toe of the foot impact the ground at the same instant and the foot of the stance leg is rotated. Also, the system is modeled as a biped robot without knees, Figure 1. In this case, there are seven DOF (two DOF on the Y-Z plane, two DOF for each leg and the DOF of the torso). The dynamic equation is given by:

$$M_e(q_e)\ddot{q}_e + C_e(q_e, \dot{q}_e)\dot{q}_e + g_e(q_e) = \tau_e + \delta F_{ext}, \tag{6}$$

where $q_e = [q_{e_1} \;\; q_{e_2} \;\; q_{e_3} \;\; q_{e_4} \;\; q_{e_5} \;\; y \;\; z]^T$, y and z are the position coordinates of the toe of the stance leg, and δF_{ext} are the external forces acting on the robot in the contact points.
It is assumed that the collision occurs during an infinitesimal period of time. The external forces in the impact moment can be represented by impulses. These impulsive forces generate an instantaneous change of joint velocities, but the positions remain the same. In this case the torques given by the actuators are not impulsive and can be neglected. Under these conditions, integrating (6) during the impact duration we obtain:

$$M_e(q_e)(\dot{q}_e^+ - \dot{q}_e^-) = F_{ext}, \tag{7}$$

where F_{ext} are the impulsive forces, and $\dot{q}_e^+$ and $\dot{q}_e^-$ are the joint velocities just after and before the impact, respectively. The joint positions do not change during the impact, then $q_e^+ = q_e^-$.
It is also assumed that the stance leg lifts from the ground without interaction, no external forces are applied at its contact point. In this case, the external forces, F_{ext}, contain only the forces acting on the heel and toe of the foot of the swing leg. Let Ψ_c and Ψ_d be the vectors of position coordinates of the heel and the toe, respectively. Hence:

$$F_{ext} = [E_c^T(q_e) \;\; E_d^T(q_e)] \begin{bmatrix} F_{c_T} \\ F_{c_N} \\ F_{d_T} \\ F_{d_N} \end{bmatrix}, \tag{8}$$

where

$$E_c(q_e) = \frac{\partial \Psi_c}{\partial q_e}, \quad E_d(q_e) = \frac{\partial \Psi_d}{\partial q_e}, \tag{9}$$

and F_{c_T}, F_{c_N}, F_{d_T}, and F_{d_N} are the tangential and normal forces applied on the heel and on the toe. An additional set of four equations is obtained from the condition that the heel and the toe of the swing leg can not move after the impact, $d/dt\Psi_c(q_e) = (\partial \Psi_c/\partial q_e)\dot{q}_e^+ = 0$ and $d/dt\Psi_d(q_e) = (\partial \Psi_d/\partial q_e)\dot{q}_e^+ = 0$, that is:

$$E_c(q_e)\dot{q}_e^+ = 0, \quad E_d(q_e)\dot{q}_e^+ = 0. \tag{10}$$

From (7) and (10):

$$\begin{bmatrix} M_e(q_e) & -E_c(q_e)^T & -E_d(q_e)^T \\ E_c(q_e) & 0 & 0 \\ E_d(q_e) & 0 & 0 \end{bmatrix} \begin{bmatrix} \dot{q}_e^+ \\ F \end{bmatrix} = \begin{bmatrix} \dot{q}_e^- \\ 0 \end{bmatrix}, \tag{11}$$

with $F = [F_{c_T} \;\; F_{c_N} \;\; F_{d_T} \;\; F_{d_N}]^T$. The value of $\dot{q}^+$ is expressed in terms of $\dot{q}_e^+$ by:

$$\dot{q}^+ = [\dot{q}_{e_1}^+ \;\; \dot{q}_{e_2}^+ \;\; \dot{q}_{e_3}^+ \;\; \dot{q}_{e_4}^+ \;\; 0 \;\; \dot{q}_{e_5}^+]^T. \tag{12}$$

After the impact, the swing leg becomes the stance leg and vice-versa. Hence, a coordinate transformation is needed to reinitialize the System (3). Considering $x = [q^T \ \ \dot{q}^T]^T$, the transformation can be given by

$$x = \Delta(x), \tag{13}$$

where

$$\Delta(x) = \begin{bmatrix} \pi \\ -q_6 \\ (q_1 + q_2 + q_3 - \pi + q_6) \\ (-2\pi - q_4) \\ 0 \\ -q_2 \\ 0 \\ -\dot{q}_6 \\ (\dot{q}_1 + \dot{q}_2 + \dot{q}_3 + \dot{q}_6) \\ -\dot{q}_4 \\ -\dot{q}_2 \end{bmatrix}. \tag{14}$$

3. Robust Dynamic Walking Control

The main problem on passive walking consists on finding a stable limit cycle without actuation of the joints for a given ground slope. However, stable limit cycles cannot be found for the biped robot considered in this paper without a loop of control be applied to the torso. In this way, PD controllers are used to keep the torso in a fixed position with relation to the horizontal line, that is, the absolute angle, $\theta_4 = q_1 + q_2 + q_3$, is controlled. The foot of the swing leg must also be controlled to reach the ground surface parallel to it at the impact instant to guarantee that the toe and the ankle touch the ground in the same time. In this case, the absolute angle $\theta_6 = q_1 + q_2 + q_4 + q_5 + q_6$, must be zero, $\theta_6^d = 0$. The PD controllers are given by:

$$\begin{aligned} \tau_4 &= K_{P_4}(\theta_4^d - \theta_4) - K_{D_4}\dot{\theta}_4, \\ \tau_6 &= K_{P_6}(\theta_6^d - \theta_6) - K_{D_6}\dot{\theta}_6, \end{aligned} \tag{15}$$

where K_{P_4}, K_{D_4}, K_{P_6}, and K_{D_6} are proportional and derivative gains, and q_4^d and q_6^d are the desired joint position for the torso and the foot of the swing leg, respectively.
In order to guarantee the passive walking at any ground slope, including zero inclination, a gravity compensation control developed by Spong & Bhatia (2003) is used. The key idea is to consider the existence of an initial condition $x(\phi_0) = [q_1(0) \ \ q_2(0) \ \cdots \ q_6(0) \ \ \dot{q}_1(0) \ \cdots \ \dot{q}_6(0)]^T$ such that, with only the PD controllers described above, a limit cycle is found for ground slope ϕ_0. Now suppose that the desired slope is ϕ. Let $\beta = \phi_0 - \phi$, R_β be the rotation defined by angle β and $P(\theta)$ the potential energy, where θ is the absolute joint position vector. In the robot configuration space the representation of angle β is given by

$$R_\beta(\theta) = \begin{bmatrix} \theta_1 - \beta \\ \vdots \\ \theta_6 - \beta \end{bmatrix}. \tag{16}$$

Now, defining $P_\beta(\theta) = P(R_\beta(\theta))$ and

$$g_\beta = \frac{\partial P_\beta(\theta)^T}{\partial \theta}, \tag{17}$$

the feedback control law is given by

$$\tau = B^{-1}(g(\theta) - g_\beta(\theta)). \tag{18}$$

This control law allows the biped robot to perform a limit cycle for ground slope ϕ, considering as initial condition $x(\phi) = [q_1(0) + \beta \;\; q_2(0) \;\; \cdots \;\; q_6(0) \;\; \dot{q}_1(0) \;\; \cdots \;\; \dot{q}_6(0)]^T$.

3.1 Nonlinear $\mathcal{H}_\infty$ control

In this work, nonlinear $\mathcal{H}_\infty$ control is applied to biped robots to increase the basin of attraction of the limit cycle and the robustness against disturbances. The proposed controller is based on design procedures developed for LPV systems. This approach provides a systematic way, using solutions based on Linear Matrix Inequalities (LMI), to design controllers that satisfy the $\mathcal{L}_2$ gain condition Wu et al. (1996). The nonlinear dynamics of the biped robot is represented as a LPV system whose parameters are in function of the state ($\rho(x)$), namely, quasi-LPV representation.
Consider the system:

$$\begin{bmatrix} \dot{x} \\ z_1 \\ z_2 \end{bmatrix} = \begin{bmatrix} A(\rho) & B_1(\rho) & B_2(\rho) \\ C_1(\rho) & 0 & 0 \\ C_2(\rho) & 0 & I \end{bmatrix} \begin{bmatrix} x \\ w \\ u \end{bmatrix}, \tag{19}$$

where x is the state vector, u is the control input vector, w is the external input vector, z_1 and z_2 are the output variables, and ρ is the parameter varying vector.
To present $\mathcal{H}_\infty$ performance the closed loop system need to satisfy the $\mathcal{L}_2$ gain condition given by:

$$\int_0^T \|z\|^2 \, \mathrm{d}t \leq \gamma^2 \int_0^T \|w\|^2 \, \mathrm{d}t. \tag{20}$$

If it is possible to find a solution $X(\rho) > 0$ to the following set of LMIs:

$$\begin{bmatrix} E(\rho) & X(\rho)C_1^T(\rho) & B_1(\rho) \\ C_1(\rho)X(\rho) & -I & 0 \\ B_1^T(\rho) & 0 & -\gamma^2 I \end{bmatrix} < 0 \tag{21}$$

where

$$E(\rho) = -\sum_{i=1}^{m} \pm \left(\nu_i \frac{\partial X}{\partial \rho_i} \right) - B_2(\rho)B_2^T(\rho) + \widehat{A}(\rho)X(\rho) + X(\rho)\widehat{A}(\rho)^T$$

and $\widehat{A}(\rho) = A(\rho) - B_2(\rho)C_2(\rho)$, then, the closed loop system has $\mathcal{L}_2$ gain $\leq \gamma$ under the state feedback law

$$u = -(B_2(\rho)X^{-1}(\rho) + C_2(\rho))x.$$

Hence, it is need to solve a set of parametric LMIs, (21), that is an infinitesimal convex optimization problem. Fortunately, a practical scheme using basis functions for $X(\rho)$ and griding the parameter set was developed in Wu et al. (1996) to solve this problem.
The quasi-LPV representation we are considering in this chapter for biped robots is shown in the following. The hybrid control strategy proposed in the next section considers that the

nonlinear $\mathcal{H}_\infty$ control is applied in the two sub-phases of the movement before the knee strike. For the sub-phase before the foot rotation, the system is considered fully-actuated since the first joint value (q_1) is fixed. It is considered the following dynamic equation with the inclusion of a disturbance vector d, corresponding to external disturbance and parametric uncertainties:

$$M_{aa}(q_a)\ddot{q}_a + C_{aa}(q_a, \dot{q}_a)\dot{q}_a + g_a(q_a) = \tau_a + d, \tag{22}$$

where $q_a = [q_2 \;\; q_3 \;\; q_4 \;\; q_5 \;\; q_6]^T$ are the active joints, and $M_{aa}(q_a)$, $C_{aa}(q_a, \dot{q}_a)$, $g_a(q_a)$, and τ_a are the corresponding partitions of the dynamic matrices.
Define the state as the composition of the trajectory tracking error and its derivative as:

$$\widetilde{x} = \begin{bmatrix} \dot{q}_a - \dot{q}_a^d \\ q_a - q_a^d \end{bmatrix} = \begin{bmatrix} \dot{\widetilde{q}}_a \\ \widetilde{q}_a \end{bmatrix}. \tag{23}$$

From (22) and (23), the biped robot state space equation is given by

$$\dot{\widetilde{x}} = A(q_a, \dot{q}_a)\widetilde{x} + B_1 w + B_2 u, \tag{24}$$

with

$$A(q_a, \dot{q}_a) = \begin{bmatrix} -M_{aa}^{-1}(q_a)C_{aa}(q_a, \dot{q}_a) & 0 \\ I & 0 \end{bmatrix}, \quad B_1 = \begin{bmatrix} I \\ 0 \end{bmatrix},$$
$$B_2 = \begin{bmatrix} I \\ 0 \end{bmatrix}, \quad w = M_{aa}^{-1}(q_a)d,$$
$$u = M_{aa}^{-1}(q_a)(\tau_a - M_{aa}(q_a)\ddot{q}_a^d - C_{aa}(q_a, \dot{q}_a)\dot{q}_a^d - g_a(q)).$$

The applied torque is computed as

$$\tau_a = M_{aa}(q_a)(\ddot{q}_a^d + u) + C_{aa}(q_a, \dot{q}_a)\dot{q}_a^d + g_a(q_a). \tag{25}$$

For the sub-phase after the foot rotation and before the knee strike, the system is underactuated since no torque is applied to the first joint and it is free. In this work, it is proposed to control only the active joints in this phase, considering the dynamic coupling with first joint and its dynamics. The following dynamic equation is used to design the quasi-LPV controller:

$$\bar{M}(q)\ddot{q}_a + \bar{C}(q, \dot{q})\dot{q}_a + \bar{D}(q, \dot{q})\dot{q}_1 + \bar{g}(q_a) = \tau_a + \bar{d}. \tag{26}$$

where $\bar{M} = M_{aa} - M_{a1}{M_{11}}^{-1}M_{1a}$, $\bar{C} = C_{aa} - M_{a1}{M_{11}}^{-1}C_{1a}$, $\bar{D} = C_{a1} - M_{a1}{M_{11}}^{-1}C_{11}$, $\bar{g} = g_a - M_{a1}{M_{11}}^{-1}g_1$, and $\bar{d}$ are the external disturbances and parametric uncertainties. Following the steps described above, a quasi-LPV representation of the biped robot, similar to (24), can be found for this sub-phase of the movement.

3.2 Hybrid Control

The PD controllers and the gravity compensation controller provide a stable walking for different ground slopes for initial positions close to the limit cycle. However, the basin of attraction of a limit cycle must be large enough to provide the system robustness against disturbances, parametric uncertainties and terrain variations. The controllers presented above are combined to produce a robust dynamic walking Bhatia & Spong (2004).

The minimum distance between the current position to the limit cycle is computed and compared to an adjustable value C, corresponding to the limit cycle basin of attraction. The minimum distance is given as

$$\bar{d} = min_i||q - q_r(i)||, \tag{27}$$

where $q_r(i)$ are discrete points on the limit cycle.
If the distance of the initial position limit cycle is lower than C, the system converges to the limit cycle. If the trajectory leaves the basin of attraction, that is, the value of $\bar{d}$ is greater than C, a control strategy based on the nonlinear $\mathcal{H}_\infty$ controller is used to come back the system to the basin of attraction as shown in Figure 3.

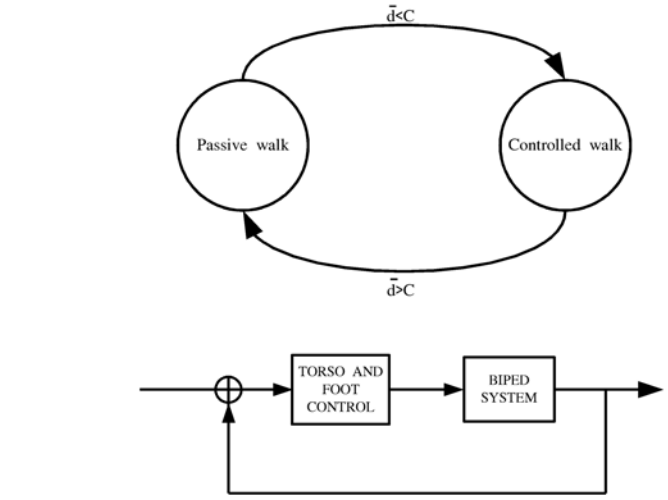

(a) Passive Diagram

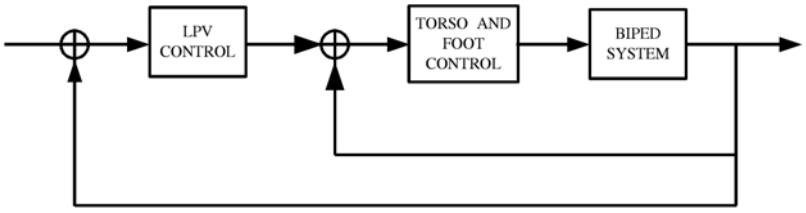

(b) Controlled Diagram

Fig. 3. Hybrid Control Strategy.

The changing point between the nonlinear $\mathcal{H}_\infty$ controller and when there is not trajectory tracking controllers (gravity compensation and PD ones) must be chosen to guarantee a smooth and natural walking. Considering the walking cycle, it is chosen the instant when

the knee strike as been this point. At this moment the swing leg is ahead the stance leg. The desired trajectory, q^d, between the position where the biped leaves the basin of attraction and the position of the knee strike is defined in this work as a 5-th polynomial, with duration corresponding to the remaining time to the impact.
Since the third sub-phase (after the knee strike and before the ground collision) is very short in the limit cycle, the nonlinear $\mathcal{H}_\infty$ controller is applied only before the knee strike. If the biped robot leaves the basin of attraction after the knee strike, only the PD controllers are used until the ground collision, and then, the nonlinear $\mathcal{H}_\infty$ controller is applied from this point until the next knee strike.

4. Results

In this section, it is presented the limit cycle for the bidimensional biped robot with feet described in Section 2 and the simulated results obtained from the implementation of the proposed hybrid control strategy. Using the Newton-Raphson method and considering a ground slope $\phi = 3^\circ$, the initial conditions to the limit cycle is given by

$$x(\phi) = \begin{bmatrix} \pi & -1.30 & -0.55 & -3.89 & 0 & 1.52 & 0 & -1.22 & 2.09 & 0.34 & 0.34 & -1.33 \end{bmatrix}^T.$$

The values used to find the solution, and the values used thorough this section, are

$$K_{P_4} = 150, \quad K_{D_4} = 100, \quad K_{P_6} = 80 \quad \text{e} \quad K_{D_6} = 10,$$

for the gains of the PD controllers, and $\theta_4^d = 80^\circ$ and $\theta_6^d = 0^\circ$, for the desired joint positions. The reference position to the trunk, θ_4^d, was selected closer to the human trunk position for a walking ahead movement. The foot rotation instant is properly adjusted through K_0 and K_M of the torsional spring on the ankle (2). For this case they were chosen as

$$K_0 = -10 \quad \text{and} \quad K_M = 30.$$

With the above values, it is found a walking cycle close to the human being with the foot rotation occurring after the swing leg to pass the normal to the ground surface and before the knee strike, which occurs just before the ground collision of the swing leg. The joint trajectories as function of the time are shown in Figure 4 and the limit cycles for the joints are shown in Figure 5, where each number in the limit cycles represents a pose of the robot during the step. These points are described below and shown in Figure 6, where the green leg is the support one and the red leg is the stance one:

1. Beginning of the limit cycle: support leg in front of the swing leg;
2. Intermediary point of the swing phase, before the foot rotation: support foot parallel to the ground;
3. Beginning of the foot rotation around the toe;
4. Intermediary point of the swing phase, before the knee strike: angle of the shank is negative ($q_5 < 0$);
5. Knee strike: angle of the shank is zero and the swing leg is straight;
6. Collision of the swing foot with the ground: support leg in the back of the swing leg.

The limit cycle found is stable. This characteristic can be verified computing the eigenvalues of the Jacobian matrix, J, obtained at the last Newton-Raphson method iteration. It is observed that the eigenvalues of J are all within the unitary circle of the complex plane, showing the stability. However, the maximum absolute value of the eigenvalues of J is given by: $max|\lambda(J)| = 0,99411$, that is, the limit cycle has a low convergence rate.

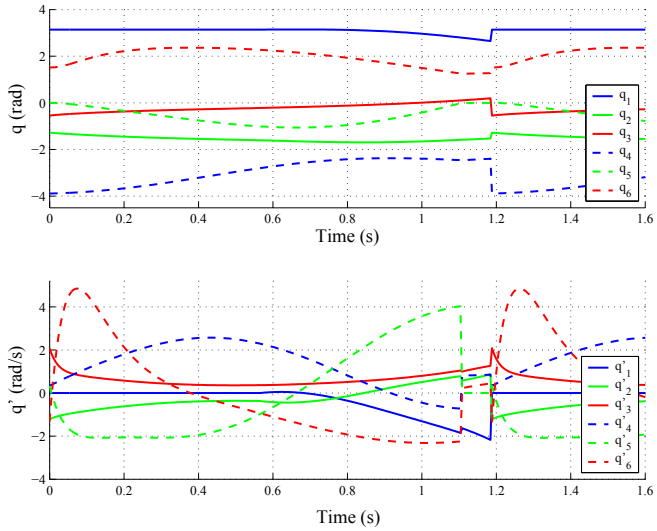

Fig. 4. Joint position and velocity time variations.

4.1 Nonlinear $\mathcal{H}_\infty$ Control

To apply the algorithm described in Section 3.1, the parameters $\rho(\tilde{x})$ are chosen as been the states representing only the position errors of the joints 2, 3, and 4 ($\widetilde{q}_2$, $\widetilde{q}_3$, and $\widetilde{q}_4$, respectively). This simplification is considered to alleviate the computational effort to find the solution for the set of LMIs (21). This is possible since the influence of the other states is small on the computation of the dynamic matrix $A(q_a, \dot{q}_a)$. Figure 7 shows the value of $||A(q_a, \dot{q}_a)||$ for a variation of each joint within its operation range. Hence, $m = 3$ and:

$$\rho(\tilde{x}) = [\widetilde{q}_2 \;\; \widetilde{q}_3 \;\; \widetilde{q}_4]^T.$$

In order to find the solution for the LMIs, the compact set where the parameters vary is defined as $\rho \in \; [-0.3, 0.3]rad \times [-0.4, 0.4]rad \times [-0.8, 0.8]rad$ and divided in ($L = 3$). Also the parameter variation rate is bounded by $|\dot{\rho}| \leq [1{,}5 \;\; 2{,}0 \;\; 3]rad/s$. These values are obtained from the limit cycle. The basis functions for $X(\rho)$ are selected as $f_1(\rho(\tilde{x})) = 1$ $f_2(\rho(\tilde{x})) = cos(\widetilde{q}_2)$, $f_3(\rho(\tilde{x})) = cos(\widetilde{q}_3)$ e $f_3(\rho(\tilde{x})) = cos(\widetilde{q}_4)$. The best attenuation level found was $\gamma = 1.5$.

4.2 Initial Conditions with Zero Velocities

Since the limit cycle has small basin of attraction, the biped robot cannot reach the limit cycle on its own from initial conditions with zero velocities. To do this, it is used the control strategy proposed in Section 3.2. The nonlinear $\mathcal{H}_\infty$ control is applied from the initial conditions to knee strike, considered as desired final position. After the knee strike, the PD and gravity compensation controllers are used. If at the beginning of the next step the initial conditions are again outside the basin of attraction, the procedure is repeated. To illustrate the effectiveness of the control strategy, consider the following initial conditions

$$x_0 = [\pi \;\; 1.3 \;\; -0.6 \;\; -3.68 \;\; 0 \;\; 1.84 \;\; 0 \;\; 0 \;\; 0 \;\; 0]^T.$$

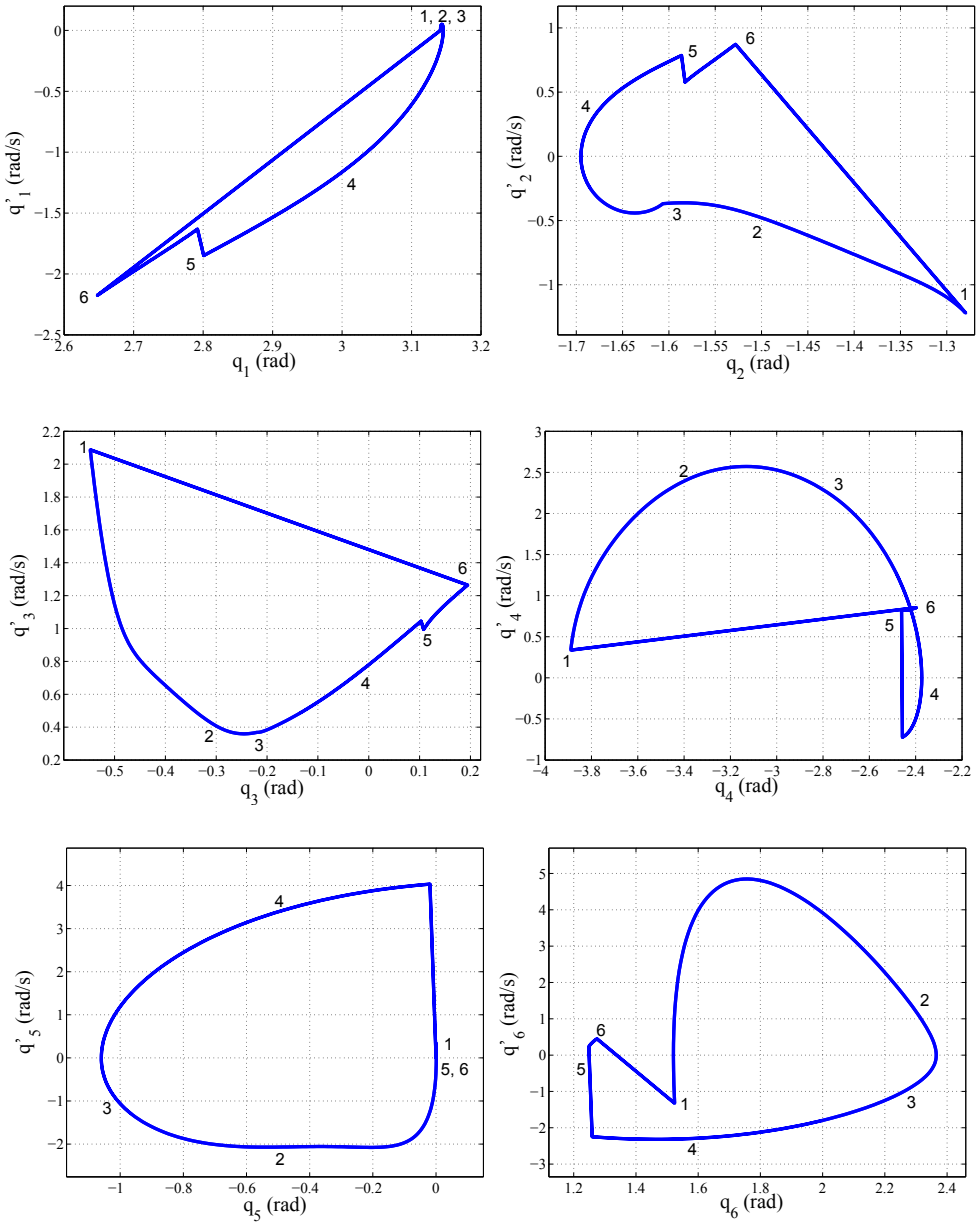

Fig. 5. Joint phase planes.

These initial conditions correspond to the legs be close to the normal to the ground surface and the feet be parallel to it. Figures 8 and 9 show the limit cycle trajectory for all joints and the joint position and velocity time variations. With the hybrid control strategy, the biped robot

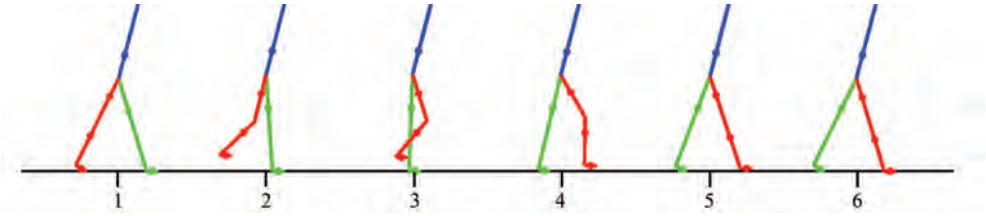

Fig. 6. Ilustration of the step in different moments.

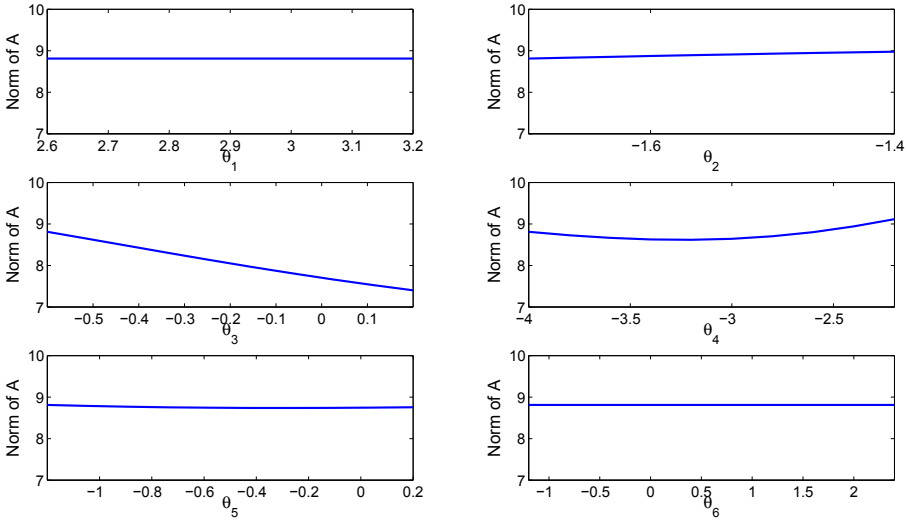

Fig. 7. Variation of $||A||$ with respect to the states.

reached the limit cycle after three steps, with a smooth trajectory from the initial conditions to the first knee strike. This example shows the basin of attraction of the limit cycle was increased for beyond the initial conditions with zero velocities with the application of the nonlinear $\mathcal{H}_\infty$ controller.

4.3 Disturbance Rejection

As seen before, the basin of attraction is small when only the PD and gravity compensation controllers are acting. Hence, even little disturbances can generate gait instability. In this section, the hybrid control strategy is used to give robustness against disturbances. In the example shown, the biped robot starts from the limit cycle initial condition, $x(\phi)$, with only the PD and gravity compensation controllers. External disturbances composed of normal and sine functions, as described in (28), are applied to the variable robot joints. At $t_f = 0,1$ s, occurs the maximum peak of the disturbance.

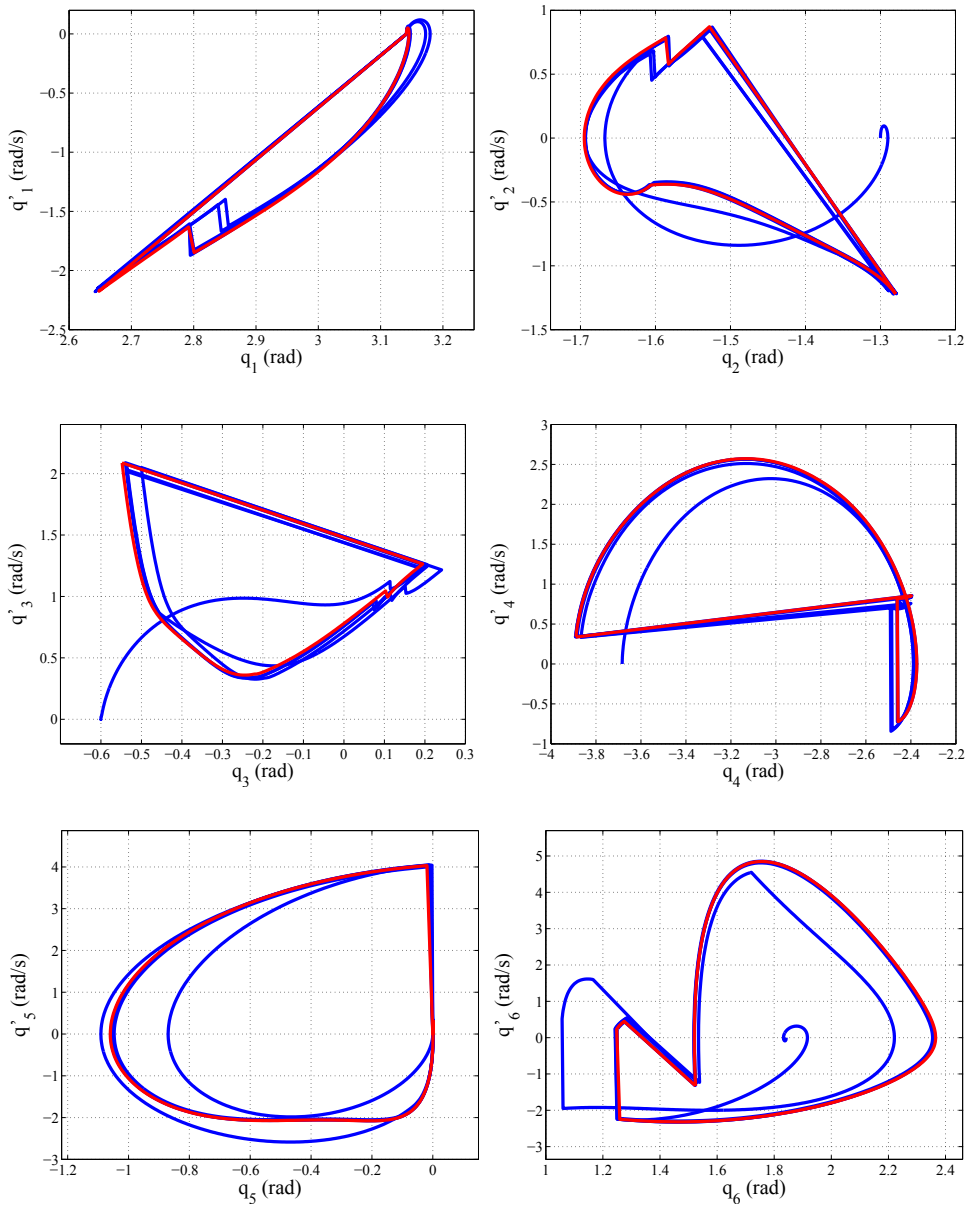

Fig. 8. Phase plane of the limit cycles with zero inicial velocities.

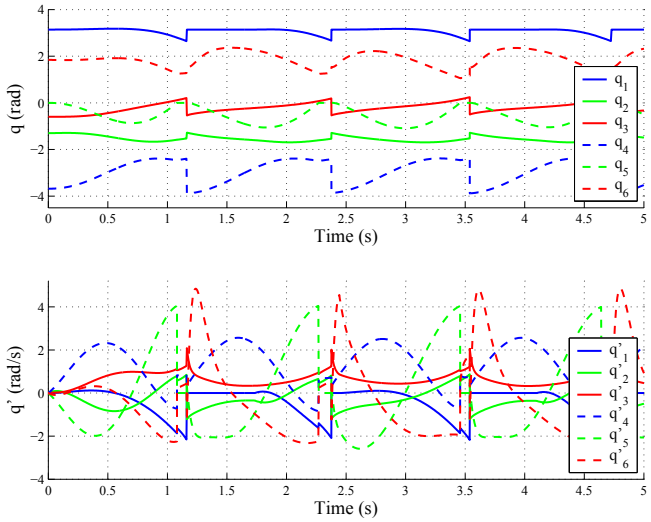

Fig. 9. Joint position and velocities with zero inicial velocities.

$$d = \begin{bmatrix} 0 \\ 0,24e^{\frac{-(t-t_f)^2}{2\sigma^2}} sin(7,2\pi t) \\ 0,18e^{\frac{-(t-t_f)^2}{2\sigma^2}} sin(5,4\pi t) \\ 0,12e^{\frac{-(t-t_f)^2}{2\sigma^2}} sin(3,6\pi t) \\ 0,012e^{\frac{-(t-t_f)^2}{2\sigma^2}} sin(3,6\pi t) \\ 0,012e^{\frac{-(t-t_f)^2}{2\sigma^2}} sin(3,6\pi t) \end{bmatrix} \tag{28}$$

The value of C, the constant that indicates the basin of attraction size, is empirically obtained from simulations with different initial conditions. In this example, $C = 0,15$. Figures 10 and 11 show the results obtained. With the disturbance application, the robot leaves the basin of attraction at the beginning of the second step at $t = 1,25$ s, instant where the control changes to the nonlinear $\mathcal{H}_\infty$ controller. It is then computed the joint desired trajectory considering as desired final position the knee strike position, with duration time corresponding to the remaining time to the impact. Note that after the knee strike at the second step, the robot does not leave any more the basin of attraction and converges to the limit cycle. Hence, the nonlinear $\mathcal{H}_\infty$ controller leads back the robot trajectory to the basin of attraction in only one step, showing the robustness of the adopted control strategy. Note also from Figure 11 that the trajectory performed by the robot during the nonlinear $\mathcal{H}_\infty$ control application is close to the limit cycle trajectory.

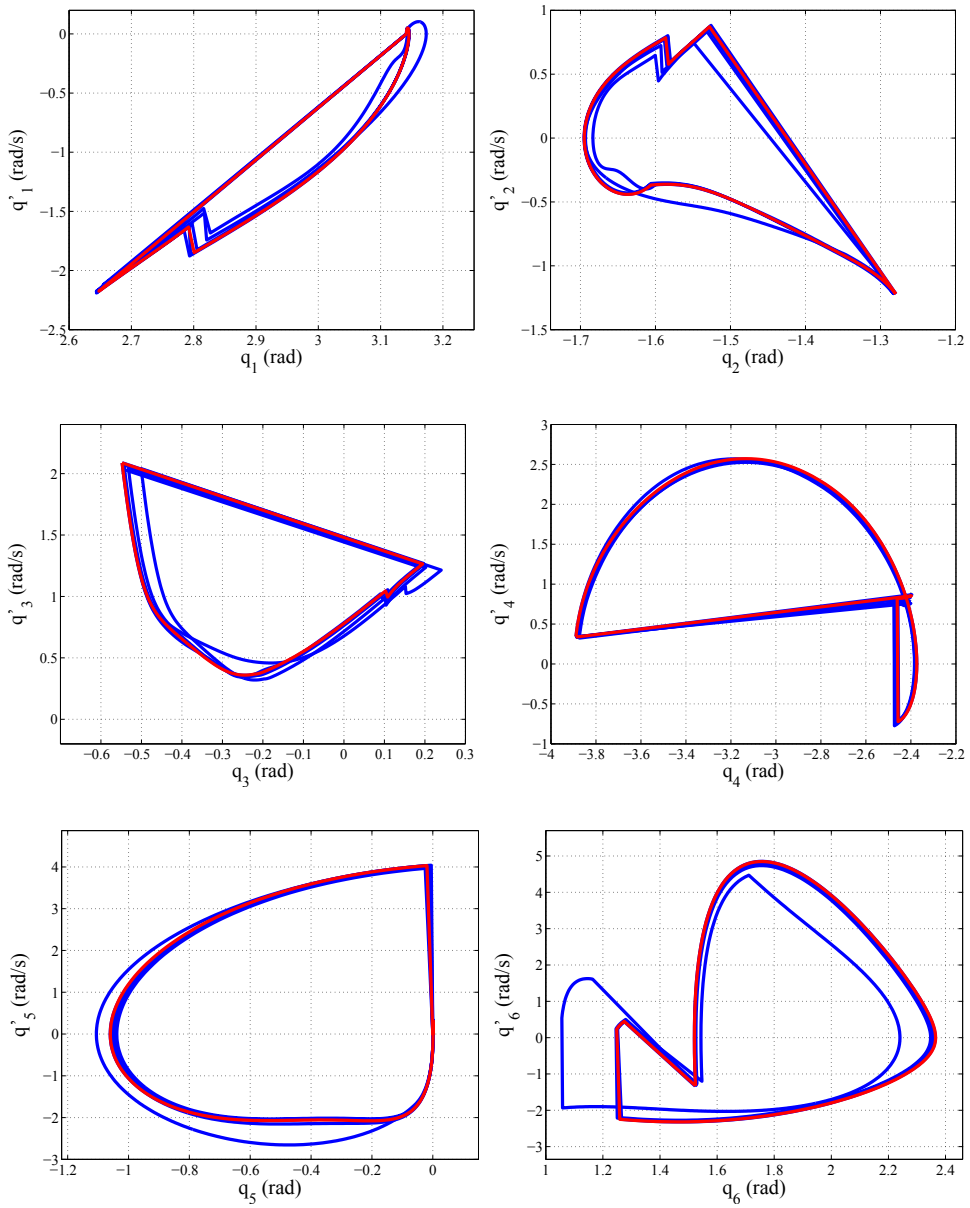

Fig. 10. Phase plane with disturbance rejection.

5. Conclusions

In this chapter, a stable limit cycle is found for a biped robot with torso, knees, and feet. However, the basin attraction is extremely small. To increase it, a control strategy based on

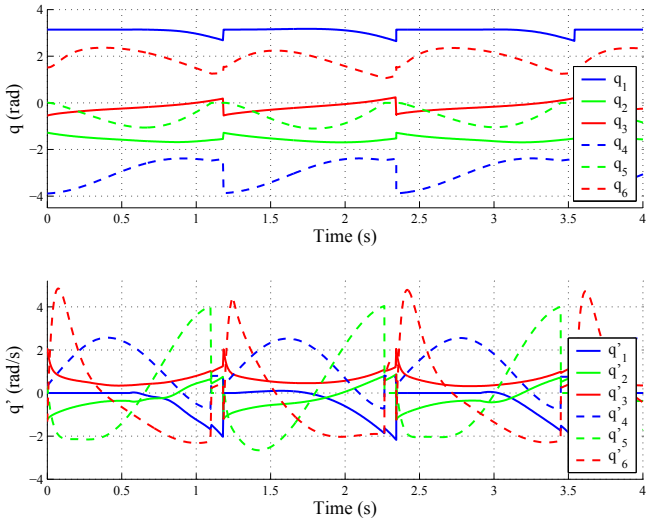

Fig. 11. Joint position and velocity time variations with disturbance rejection.

nonlinear $\mathcal{H}_\infty$ control and on a suitable choice of the switch point between the passive walking and the controlled trajectory is proposed. The results show that the basin of attraction is increased with the adopted strategy, for example, to beyond the initial conditions with zero velocities. In addition, system robustness is verified with the fast convergence to the stable gait, only one step, after the application of external torque disturbances.

6. References

Asano, F., Luo, Z.-W. & Yamakita, M. (2005). Biped gait generation and control based on a unified property of passive dynamic walking, *IEEE Transactions on Robotics* **21**(4): 754–762.

Asano, F. & Yamakita, M. (2001). Virtual gravity and coupling control for robot gait synthesis, *Transactions on Systems, Man and Cybernetics* **31**(6): 737–745.

Bhatia, G. & Spong, M. W. (2004). Hybrid control for smooth walking of a biped with knees and torso, *Institute of Electrical and Eletronics Engineers Conference on Control Applications*, Taipei, Taiwan.

Chevallereau, C., Abba, G., Aoustin, Y., Plestan, F., Westervelt, E. R., Canudas-de Wit, C. & Grizzle, J. W. (2003). Rabbit: A testbed for advanced control theory, *IEEE Control Systems Magazine* **23**(5): 57–79.

Choi, J. H. & Grizzle, J. W. (2005). Planar bipedal walking with foot rotation, *Proceedings of the 2005 American Conrtol Conference (ACC)*, Portland, Oregon, USA.

Goswani, A. (1999). Foot rotation indicator (fri) point: A new gait planning tool to evaluate postural stability of biped robots, *Proceedings of the 1999 IEEE International Conference on Robotics and Automation (ICRA)*, Detroit, Michigan, USA.

Goswani, A., Thuilot, B. & Espiau, B. (1998). A study of the passive gait of a compass-like biped robot, *International Journal of Robotics Research* **17**(12): 1282–1301.

Hirukawa, H., Kanehiro, F., Kaneko, K., Kajita, S., Fujiwara, K., Kawai, Y., Tomita, F., Hirai, S., Tanie, K., Isozumi, T., Akachi, K., Kawasaki, T., Ota, S., Yokoyama, K., Handa, H., Fukase, Y., Maeda, J., Nakamura, Y., Tachi, S. & Inoue, H. (2004). Humanoid robotics platforms developed in hrp, *Robotics and Autonomous Systems* **48**(4): 165 – 175. Humanoids 2003.

Huang, Q., Yokoi, K., Kajita, S., Kaneko, K., Arai, H., Koyachi, N. & Tanie, K. (2001). Planning walking patterns for a biped robot, *IEEE Transactions on Robotics and Automation* **17**(3): 280–289.

McGeer, T. (1990). Passive dynamic walking, *International Journal of Robotics Research* **9**(2): 62–82.

Palmer, M. L. (2002). *Sagittal Plane Characterization of Normal Human Ankle Function Across A Range Of Walking Gait Speeds, M.S. Thesis*, Massachusetts Institute of Technology, Department of Mechanical Engineering.

Siqueira, A. A. G. & Terra, M. H. (2002). Control of underactuated manipulators using nonlinear $\mathcal{H}_\infty$ techniques, *Proceedings of the 2002 IEEE Conference on Decision and Control (CDC)*, Las Vegas, Nevada, USA.

Siqueira, A. A. G. & Terra, M. H. (2004). Nonlinear and markovian $\mathcal{H}_\infty$ controls of underactuated manipulators, *IEEE Transactions on Control Systems Technology* **12**(6): 811–826.

Spong, M. W. & Bhatia, G. (2003). Further results on passivity based control of bipedal locomotion, *International Conference on Intelligent Robots and Systems*, Las Vegas, USA.

Vukobratovic, M. & Juricic, D. (1969). Contribution to the synthesis of biped gait, *IEEE Transactions on Bio-Medical Engineering* **BM-16**(1): 1–6.

Westervelt, E. R., Grizzle, J. W. & Koditschek, D. E. (2003). Hybrid zero dynamics of planar biped walkers, *IEEE Transactions on Automatic Control* **48**(1): 42–56.

Wu, F., Yang, X. H., Packard, A. & Becker, G. (1996). Induced $\mathcal{L}_2$-norm control for LPV systems with bounded parameter variation rates, *International Journal of Robust and Nonlinear Control* **6**(9-10): 983–998.